

Calcium carbonate pump during Quaternary glacial cycles in the South China Sea

LIU Zhifei, XU Jian, TIAN Jun & WANG Pinxian

Laboratory of Marine Geology, Tongji University, Shanghai 200092, China

Correspondence should be addressed to Liu Zhifei (e-mail: lzhifei@online.sh.cn)

Abstract The preservation and dissolution of calcium carbonate (namely calcium carbonate pump) controls the pH of seawater in global oceans by its buffer effect, and in turn plays a significant role in global changes in atmospheric CO₂ concentration. The results from measured carbonate contents over the past 2 Ma at ODP Site 1143 in the South China Sea provide high-resolution records to explore the process of the calcium carbonate pump during Quaternary glacial cycles. The results indicate statistically that the highest carbonate accumulation rate leads the lightest δ¹⁸O by about 3.6 ka at transitions from glacial to interglacials, and that the strongest carbonate dissolution lags the lightest δ¹⁸O by about 5.6 ka at transitions from interglacials to glacial. The calcium carbonate pump releases CO₂ to the atmosphere at the glacial-interglacial transitions, but transports atmospheric CO₂ to deep sea at the interglacial-glacial transitions. The adjustable function of the calcium carbonate pump for the deep-sea CO₃²⁻ concentration directly controls parts of global changes in atmospheric CO₂, and contributes the global carbon cycle system during the Quaternary.

Keywords: calcium carbonate pump, biological pump, glacial cycles, Quaternary, South China Sea, Ocean Drilling Program (ODP).

DOI: 10.1360/02wd0336

The most remarkable feature of climate changes during the Quaternary on the Earth is glacial cycles. During cold glacial periods, large continental ice sheets covered much of the polar Northern Hemisphere. During warm interglacial periods, Northern Hemisphere glaciation wanes drastically. The ultimate pacing of these glacial cycles is statistically linked to cyclic changes in the orbital parameters of the Earth, known as the Milankovitch cycles^[1]. However, the energy budget effects of the orbital variations are insufficient to drive the large amplitude of the glacial cycles, and orbital variations alone do not provide an obvious cause of the rapid climate transitions evident in geological records. Positive feedbacks within the Earth's climate system must amplify orbital forcing to produce glacial cycles^[2]. Among them, the atmospheric CO₂ plays a large role over the glacial cycles^[3]. The atmospheric CO₂ concentration has varied in step with glacial-interglacial cycles^[4]. During interglacials, the atmos-

pheric partial pressure of CO₂ (pCO₂) is typically near 280 parts per million by volume (ppmv). During glacial, atmospheric pCO₂ is only 180—200 ppmv. The cause of these variations in CO₂ has been a debate on various global change studies, including carbon storage change on land^[5], ocean temperature variation^[6], calcium carbonate storage change in the ocean^[7], ocean nutrition storage change^[8], and nutrient utilization at high latitudes^[9], but any of them is not broadly accepted^[2,10]. Current attention is focused on variations in the atmospheric CO₂ concentration caused by the biological pump^[11,12].

The biological pump fixes CO₂ through the photosynthesis of phytoplankton, transports carbon to the deep sea, and results in the temporary or permanent storage of carbon. The biological pump includes two types of carbon pumps^[10,13]: organic carbon pump and calcium carbonate pump (Fig. 1). The organic carbon pump takes up dissolved inorganic carbon (mainly including aqueous CO₂, HCO₃⁻, and CO₃²⁻) and nutrients (essentially phosphate and nitrate) through the photosynthesis of phytoplankton in the euphotic zone (the uppermost 100—200 m), produces organic matter (particulate organic carbon, POC), and releases oxygen. The calcium carbonate pump, however, releases CO₂ through the production of some marine organisms' carbonate skeletons and shells (particulate inorganic carbon, PIC). Most of PIC is the calcium carbonate as calcite and aragonite. Therefore, two types of carbon pumps have different effects on the seawater's carbonate system^[10,13]. In the surface ocean, the organic carbon pump reduces pCO₂, whereas the calcium carbonate pump increased pCO₂. In the deep-sea ocean, a part of organic carbon becomes oxidized, increasing CO₂ (namely respired CO₂), but the dissolution of calcium carbonate takes up CO₂ (Fig. 1).

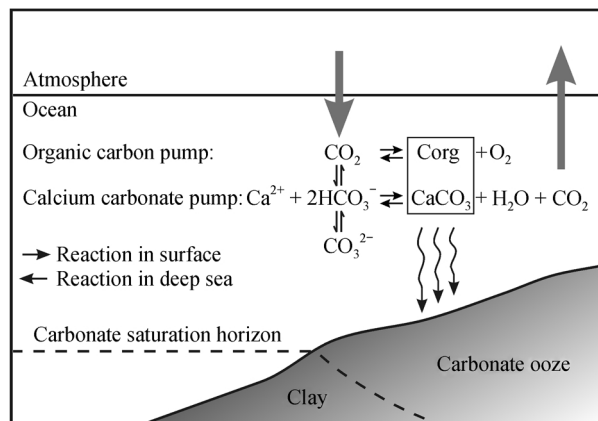


Fig. 1. Aspects of the ocean's biological pump. Dissolved inorganic carbon exists in seawater as aqueous CO₂, HCO₃⁻, and CO₃²⁻. The organic carbon pump is a sink for atmospheric CO₂, whereas the calcium carbonate pump is a source of CO₂ on short time scales. Modified after ref. [10].

Previous studies on atmospheric CO₂ responses of the biological pump were focused on the organic carbon pump, a process fixing CO₂ through the photosynthesis of phytoplankton^[8,11,12], but a few efforts were performed on the calcium carbonate pump, a major process controlling the pH of the ocean^[10]. The dissolved inorganic carbon as a buffer controls the pH of seawater in global oceans, and in turn plays a significant role to global changes in the atmospheric CO₂ concentration^[10,14–16]. The strongest dissolution events, which occurred mainly at transitions from interglacials to glacials during the Late Pleistocene to Holocene, were found firstly at sediment cores in Indian-Pacific Oceans^[17,18]. In a study of sediments from the Indian Ocean's 90°E ridge, times of pronounced dissolution happened at the interglacial to glacial boundaries of isotope stages 5/4, 7/6, 9/8, and 13/12 in the past 500 ka^[18]. Those events then were confirmed in the deep-sea carbonate sediments in the equatorial Pacific^[19,20] and Atlantic^[21,22]. Furthermore, the excess CaCO₃ dissolution was estimated as about 28 g/cm² for each transition event at isotope stages 11/10, 9/8, and 7/6 boundaries in the equatorial Pacific^[14]. This result is consistent with those expected from seawater pH shifts reconstructed based on boron isotope measurements and from bottom seawater CO₃²⁻ concentrations measured from foraminiferal shell weight^[15]. Therefore, the strong carbonate dissolution events at the interglacial-glacial transitions largely increase the CO₃²⁻ concentration and the pH of the seawater, and in turn force the onset of glaciation^[14,23]. If strong dissolution events occur at the onset of glacial periods, then one would expect strong preservation events following each termination. Although the preservation event was found at the isotope stages 2/1 transition in the South China Sea (SCS)^[24] and in the Late Pleistocene sediments in Indian Ocean^[22], perhaps because of the Holocene record being overprinted or the deposition of CaCO₃ in coral reefs and shallow banks^[14], the investigation of preservation and dissolution events of calcium carbonate (namely calcium carbonate pump) during the Quaternary is far from enough.

The sediment cores at Site 1143 in the southern SCS, recovered during the ODP Leg 184 in 1999^[25], reveal high-resolution preservation and dissolution events of calcium carbonate over the past 2 Ma, and provide ideal materials to explore the process of the calcium carbonate pump and its effects on the global carbon cycle system. This paper presents measured results of carbonate contents, carbonate mass accumulation rate, carbonate dissolution index, and benthic foraminifer $\delta^{18}\text{O}$, and discusses the process of the calcium carbonate pump during Quaternary glacial cycles in the SCS and its effects on variations in global atmospheric CO₂ concentration.

1 Material and methods

ODP Site 1143 is located at 9°21.72'N, 113°17.11'E, at a water depth of 2772 m in the southern SCS. The core length is 510 mcd (meters composite depth) and displays continuous green or olive green clay, nannofossil, and foraminifer ooze for the upper 100 mcd, and shallower color, decreased green clay, and a few turbidite sediments developed for the lower part^[25]. The present depths of the lysocline and the CCD (carbonate compensation depth) in the SCS are about 3000 m and 3800 m, respectively^[26,27]. In the last glacial interval, however, the sea level dropped about 116 m^[28] and the CCD deepened to 4200 m^[29]. Therefore, the materials used in this study are located above the lysocline and CCD. Samples were collected at 10 cm intervals along the upper 95.02 mcd. All samples were analyzed for benthic foraminiferal $\delta^{18}\text{O}$, carbonate contents, and fragmentation of planktonic foraminifera.

Oxygen isotope analysis was conducted on the benthic foraminifer *Cibicidoides wuellerstorfi* (300–900 μm size fraction) using a Finnigan MAT 252 mass spectrometer^[30]. Data were reported relative to the Pee Dee belemnite standard with an external error of less than $\pm 0.08\%$. The age-depth relationship for Site 1143 was constructed on the basis of precise correlation with the benthic foraminiferal $\delta^{18}\text{O}$ from ODP Site 677^[31], with a temporal resolution of 2 ka^[32]. Carbonate contents were determined using the gasometric techniques^[33], which have a precision of better than $\pm 2\%$. Carbonate mass accumulation rate (MAR) was calculated from linear sedimentation rate, dry bulk density, and carbonate contents^[34], in which the dry bulk density was after the shipboard data^[25]. Statistics of fragmentation of planktonic foraminifera was took from fractions $> 150 \mu\text{m}$ to reflect various dissolution. The method assuming that each individual foraminifer test breaks up into an average of eight fragments^[20] was adopted to calculate the ratio of broken with entire tests. The software Arand^[35] was used to conduct cross-correlation analysis between benthic $\delta^{18}\text{O}$ and carbonate MAR, and between benthic $\delta^{18}\text{O}$ and foraminifer fragmentation, to reveal their general physical-phase correlations. All analyses were carried out at the Laboratory of Marine Geology, Tongji University.

2 Results and discussion

(i) Variations in carbonate MAR leads fluctuations in $\delta^{18}\text{O}$. Values of benthic $\delta^{18}\text{O}$ are records of the polar ice volume, reflecting a synchronicity of glacial cycles. The benthic $\delta^{18}\text{O}$ results of Site 1143 well correlate to SEPCMAP^[36] and other records in global oceans, and thus provide a detailed timescale for the chronostratigraphy of glacial-interglacial cycles^[30,32] (Fig. 2). Percentage of carbonate contents varies between 2% and 39%, and their curve is parallel generally to that of benthic $\delta^{18}\text{O}$ (Fig. 2), with the highest carbonate content corresponding to the

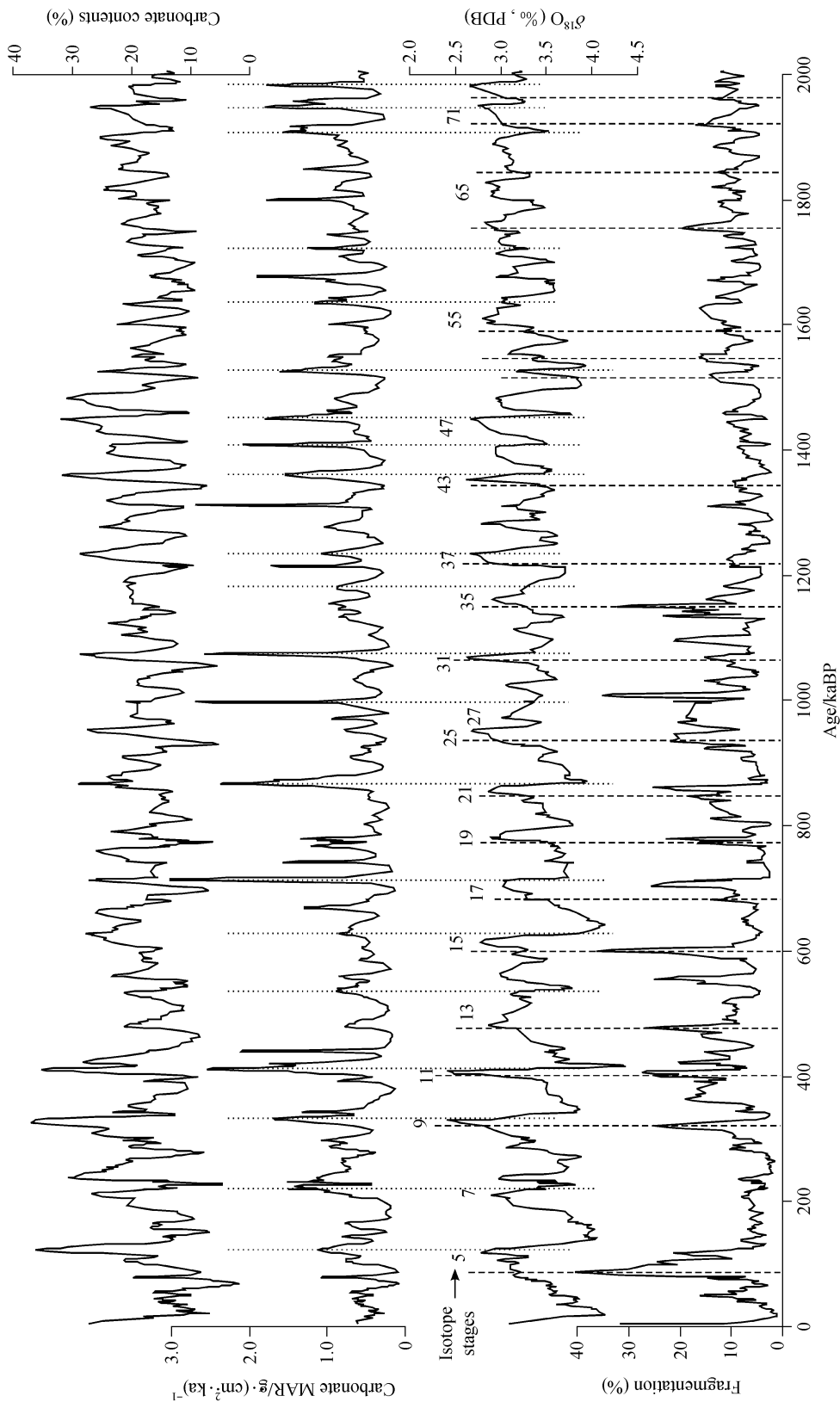


Fig. 2. Carbonate contents, carbonate MAR (mass accumulation rate), benthic foraminiferal $\delta^{18}\text{O}$, and planktonic foraminiferal fragmentation over the past 2 Ma at ODP Site 1143 in the SCS. Parallel samples were analyzed with a temporal resolution of about 2 ka. All original data were smoothed with a 3-point running average window. Data of benthic $\delta^{18}\text{O}$ and isotope stages after refs. [30, 32].

lightest $\delta^{18}\text{O}$. The pattern of the carbonate variability is characteristic of the Atlantic type^[21,37], following previous works during the Quaternary in the SCS^[38,39]. The carbonate MAR, which is corrected for dilution by terrigenous inputs, can reflect the productivity of calcium carbonate^[34]. Values of the carbonate MAR at Site 1143 varies generally within 0.2—2.0 g/cm² · ka⁻¹, with a few values higher to 3.0 g/cm² · ka⁻¹ (Fig. 2). Note that, the higher carbonate MAR generally occurred at transitions from glacial to interglacials, for examples, isotope stages 6/5, 8/7, 10/9, 12/11, 14/13, and 16/15. Thus may imply significantly increased biogenetic productivity of carbonate shells and nannofossil. Cross-correlation statistical analysis indicates that the best correlation ($r = 0.44$) of the two signals is obtained if the highest carbonate MAR leads the lightest $\delta^{18}\text{O}$ by about 3.6 ka (Fig. 3(a)).

(ii) Variations in carbonate dissolution lags fluctuations in $\delta^{18}\text{O}$. Foraminiferal fragmentation usually indicates carbonate dissolution^[18,20,34]. The fragmentation at ODP Site 1143 shows periodic dissolution events, with high values up to 40% during strong dissolution events (Fig. 2). These pronounced dissolution events occurred generally at the interglacial-glacial transitions, for examples, isotope stages 5/4, 9/8, 11/10, 13/12, and 15/14, implying increased dissolution during the settling of planktonic foraminiferal shells and from the interaction with hole water on the seafloor. Those results are consistent with carbonate records in global oceans^[14,19–22] and from numerical modeling^[13]. At the onset of last glacial period, for instance, the CO_3^{2-} concentration in seawater would have risen by $90 \pm 30 \mu\text{mol/L}$ ^[23]. To obtain this amount of CO_3^{2-} could require the dissolution of $5.3 \pm 1.8 \text{ g/cm}^2$ CaCO_3 of seafloor, or about $22 \pm 8 \text{ g/cm}^2$ of area covered with CaCO_3 -rich sediments^[14]. Cross-correlation statistical analysis confirms that the best correlation ($r = 0.42$) of the two signals is received if the strongest carbonate dissolution lags the lightest $\delta^{18}\text{O}$ by about 5.6 ka (Fig. 3(b)).

(iii) Calcium carbonate pump during glacial cycles.

The variations in carbonate MAR lead fluctuations in benthic $\delta^{18}\text{O}$, but the variations in dissolution lag benthic $\delta^{18}\text{O}$, indicating a potential mechanism of changes in calcium carbonate in seawater during the Quaternary glacial cycles. The results from Site 1143 in the SCS indicate that the carbonate MAR increased at the glacial-interglacial transitions. The biogenic calcification, mainly including formations of foraminiferal shells and nannofossil, was active strongly. The calcium carbonate pump transported the dissolved inorganic carbon (as aqueous CO_2 , HCO_3^- , and CO_3^{2-}) from surface to seafloor. The calcification mainly used carbon dissolved in seawater as HCO_3^- ^[13]. Two moles of HCO_3^- react with 1 mole of Ca^{2+} to pre-

cipitate 1 mole of CaCO_3 , releasing the extra mole of carbon as CO_2 and reducing the CO_3^{2-} concentration in seawater (Fig. 1). Thus, biogenic calcification is a potential source of CO_2 to the atmosphere, rather than a carbon sink^[10]. During the transitions of interglacials to glacials, the carbonate dissolution increased. To dissolve 1 mole of CaCO_3 requires 1 mole of CO_2 , and produces 2 moles of HCO_3^- , increasing the CO_3^{2-} concentration in seawater. This CaCO_3 dissolution could occur during the settling of calcitic shells through the water column, within the species body's cavities, or in sediments on the seafloor^[13]. During the last glacial Plateau region. Magnetic susceptibility correlates well period, for example, a study on the CO_3^{2-} concentration in seawater at the Ontong-Java Plateau in the western Pacific indicates that the CO_3^{2-} concentration at 3-km depth is $12 \mu\text{mol/kg}$ higher than that during the Holocene, and increases with the water depth^[15]. For this case, the calcium carbonate pump transported CO_2 to the deep sea and becomes a sink of the atmospheric CO_2 . Therefore, the calcium carbonate pump ultimately affects the CO_3^{2-} concentration and the pH in seawater. The CO_3^{2-} concentration is proportional to the pH and inversely proportional to the CO_2 concentration^[10]. This is intuitively obvious: during interglacials, relatively lower CO_3^{2-} concentration and pH in seawater and relatively high atmospheric CO_2 concentration produce relatively higher global temperature because of the greenhouse effect; during glacials, relatively high CO_3^{2-} concentration in seawater made relatively lower atmospheric CO_2 concentration, and in turn relatively low global temperature.

(iv) Implications for global atmospheric pCO_2 .

According to the mechanism of calcium carbonate pump during the glacial cycles, changes in the CO_3^{2-} concentration must play a significant role in atmospheric pCO_2 variations^[22]. The questions are “when” and “by how”. The carbonate records from Site 1143 can address some of the two questions. The carbonate contents during the last three glacial-interglacial cycles at Site 1143 in the SCS are correlated to atmospheric pCO_2 and δD variations from the Vostok ice core in Antarctic^[4] (Fig. 4), to determine effects of marine calcium carbonate pump on variations in the global atmospheric CO_2 .

The atmospheric pCO_2 at Vostok started to increase at about 600 ± 400 a after warming in the last three glacial-interglacial cycles, with an approximate 80%—100%. After the onset of glacials, the high atmospheric pCO_2 can last several thousands of years^[4,40] (Fig. 4). During termination I, the Vostok atmospheric pCO_2 and deep-sea

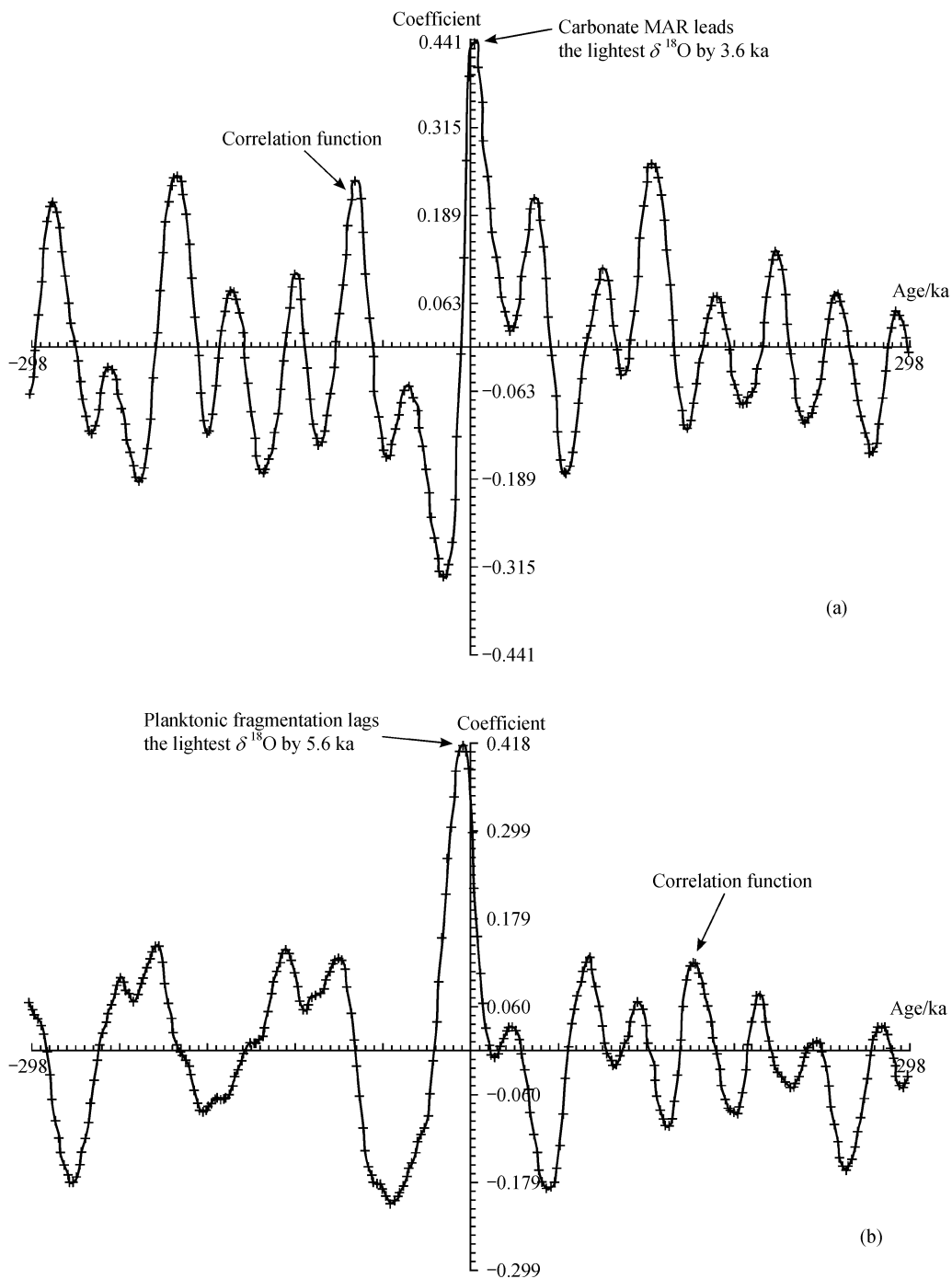


Fig. 3. Cross-correlation statistical analysis of benthic foraminiferal $\delta^{18}\text{O}$ with carbonate MAR and planktonic foraminiferal fragmentation. (a) benthic $\delta^{18}\text{O}$ with carbonate MAR; (b) benthic $\delta^{18}\text{O}$ with planktonic fragmentation. Software Arand^[35] was used to perform the cross-correlation analysis, with 150 samples for each range and about 2 ka for the temporal resolution, and in turn for a maximum of 149 samples and a time difference of 298 ka. On the coordinate, a positive time refers to a lead and a negative one refers to a lag; a positive coefficient refers to positive correlation and a negative one refers to negative correlation.

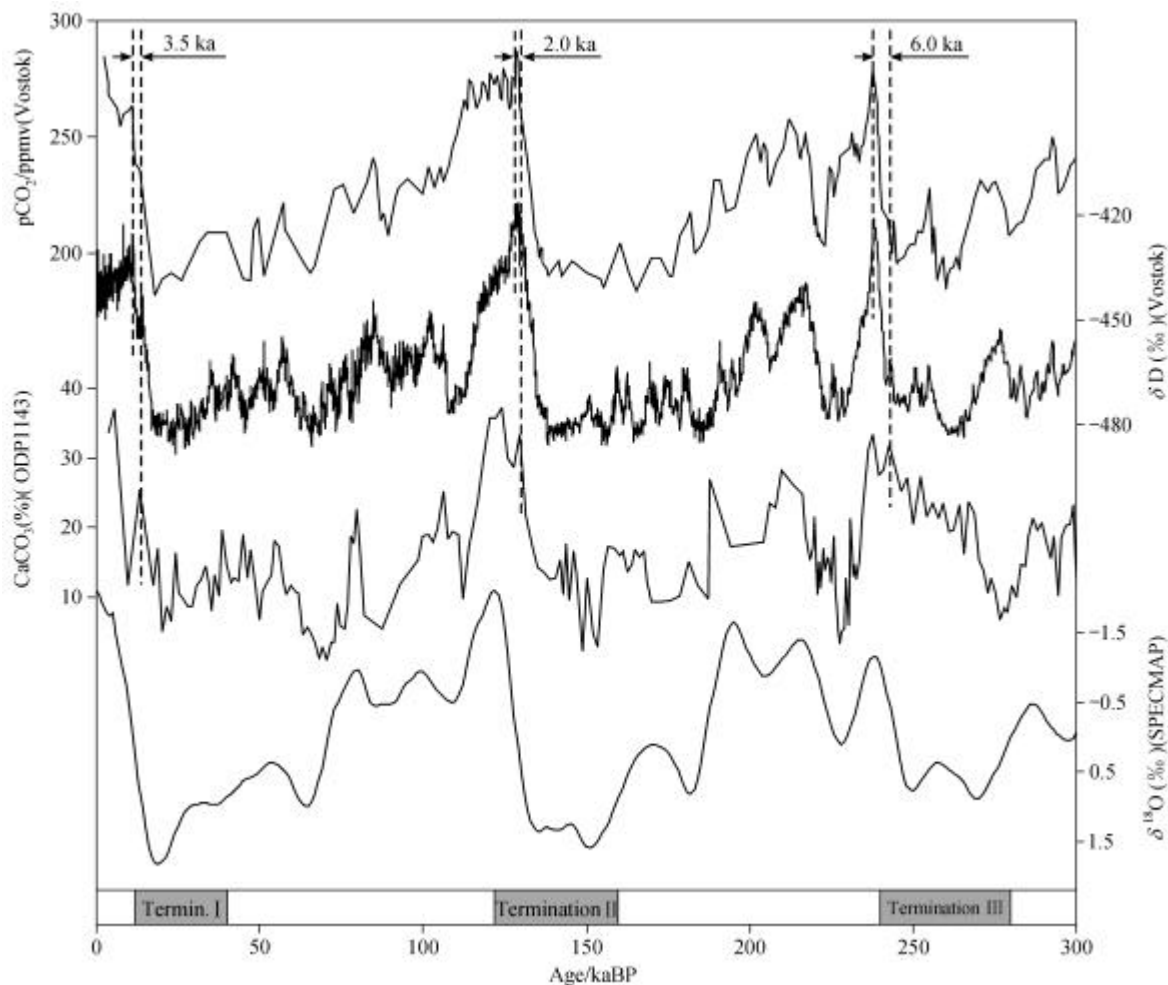


Fig. 4. Comparison of carbonate contents at ODP Site 1143 with $p\text{CO}_2$ and δD at Vostok ice core^[4] in the last three glacial-interglacial cycles. δD is a proxy of the Antarctic temperature. Note that negative values referring cold weathers. The benthic foraminiferal $\delta^{18}\text{O}$ of SPECMAP^[36] provides a history of global ice volume.

CaCO_3 increased synchronously at about 20 ka BP. The CaCO_3 reached its maximum at 14 ka BP, but the atmospheric $p\text{CO}_2$ reached its maximum at 10.5 ka BP, with a time difference of 3.5 ka. During termination II, the Vostok atmospheric $p\text{CO}_2$ started to increase at 135 ka, a short later than that of the deep-sea CaCO_3 . Similarly to the Holocene, the atmospheric $p\text{CO}_2$ reached its maximum at 128 ka BP, later than the CaCO_3 maximum by about 2.0 ka. During termination III, two signals increased synchronously at 250 ka BP. the magnitude of variations in CaCO_3 is larger than that of fluctuations in atmospheric $p\text{CO}_2$. The atmospheric $p\text{CO}_2$ reached its maximum later than CaCO_3 by about 6.0 ka. The variations in the Vostok atmospheric $p\text{CO}_2$ generally lag those of deep-sea CaCO_3 , implying a control of the marine calcium carbonate pump on parts of global changes in atmospheric CO_2 . During the onset of terminations, the productivity of biogenic calcitic

shells increased, and then the calcium carbonate pump released CO_2 to the atmosphere to improve the atmospheric $p\text{CO}_2$. After the formation of glacials, the carbonate dissolution increased, and the calcium carbonate pump transported the atmospheric CO_2 to the deep sea by the interaction between oceanic surface and atmosphere, to reduce the atmospheric $p\text{CO}_2$. Because of the buffer effect of CO_2 ^[10], the high atmospheric $p\text{CO}_2$ usually lasted several thousands of years, rather than immediately decreasing after the onset of glacials. Previous works on the CaCO_3 dissolution cycles in the equatorial Pacific^[14] suggested that the CaCO_3 dissolution events forced the onset of times of glaciation, implying a control of the calcium carbonate pump on the global atmospheric CO_2 .

However, the marine calcium carbonate pump does not completely control all variations during glacial cycles. For example, the carbonate dissolution did not increase at

the transitions of isotope stages 7/6 and 27/26 at Site 1143; similarly, the carbonate MAR did not increase at the boundaries of isotope stages 20/19 and 26/25 (Fig. 2). Those imply complicated changes in the global atmospheric CO₂. The carbon on the Earth exists as inorganic and organic types and circulates between the atmosphere, hydrosphere, lithosphere, and biosphere. The atmospheric pCO₂ is a result of those circulations. Besides the control of the marine calcium carbonate pump on the atmospheric pCO₂, organic carbon pump^[11,12] with a reversed process to the calcium carbonate pump, nutrient utilization in surface water at high latitudes^[9], and variation in carbon reservoir at continental uplift regions contribute to the global climate changes. But, this paper presents a significant aspect of the global carbon cycle.

3 Conclusions

Carbonate contents, carbonate MAR, benthic foraminiferal δ¹⁸O, and planktonic foraminiferal fragmentation were analyzed with a high resolution over the past 2 Ma at ODP Site 1143 in the South China Sea to reveal the process of calcium carbonate pump during the Quaternary glacial cycles. The results indicate statistically that the highest carbonate accumulation rate leads the lightest δ¹⁸O by about 3.6 ka at most of transitions from glacial to interglacials, implying that the higher productivity of biogenic calcitic shells produced relatively low CO₃²⁻ concentration and relatively high release of CO₂, and then relatively high atmospheric pCO₂ and global temperature. During most of glacial-interglacial transitions, the strongest carbonate dissolution lags the lightest δ¹⁸O by about 5.6 ka, indicating that stronger carbonate dissolution made the calcium carbonate pump transporting atmospheric CO₂ to the deep sea, and produced relatively high CO₃²⁻ concentration and the pH in seawater, and in turn relatively low atmospheric pCO₂ and global temperature. The adjustable function of the calcium carbonate pump for the CO₃²⁻ concentration in seawater directly controls parts of global changes in atmospheric CO₂, and contributes to the global carbon cycle system.

Acknowledgements All samples used in this study were provided by the Ocean Drilling Program (ODP), which is sponsored by the U.S. National Science Foundation (NSF) and participating countries under the management of Joint Oceanographic Institutions (JOI), Inc. This work was supported by the National Key Basic Research Development Project of China (Grant No. G2000078505) and the National Natural Science Foundation of China (Grant Nos. 49999560 and 40102010).

References

1. Hays, J. D., Imbrie, J., Shackleton, N. J., Variations in the Earth's orbit: pacemaker of the Ice Ages, *Science*, 1976, 194: 1121—1132.
2. Sigman, D. M., Boyle, E. A., Glacial/interglacial variations in at-

- mospheric carbon dioxide, *Nature*, 2000, 407: 859—869.
3. Webb, R. S., Lehman, S. J., Rind, D. H. et al., Influence of ocean heat transport on the climate of the Last Glacial Maximum, *Nature*, 1997, 385: 695—699.
4. Petit, J. R., Jouzel, J., Raynaud, D. et al., Climate and atmospheric history of the past 420,000 years from the Vostok ice core, *Antarctica*, *Nature*, 1999, 399: 429—436.
5. Adams, J. M., Faure, H., Faure-Denard, L. et al., Increases in terrestrial carbon storage from the Last Glacial Maximum to the present, *Nature*, 1990, 348: 711—714.
6. Guilderson, T. P., Fairbanks, R. G., Rubenstone, J. L., Tropical temperature variations since 20000 years ago: modulating inter-hemispheric climate change, *Science*, 1994, 263: 663—665.
7. Broecker, W., Peng, T.-H., The role of CaCO₃ compensation in the glacial to interglacial atmospheric CO₂ change, *Glob. Biogeochem. Cycles*, 1987, 1: 15—29.
8. McElroy, M. B., Marine geological controls on atmospheric CO₂ and climate, *Nature*, 1983, 302: 328—329.
9. Sarmiento, J. L., Toggweiler, J. R., A new model for the role of the oceans in determining atmospheric pCO₂, *Nature*, 1983, 308: 621—624.
10. Elderfield, H., Carbonate mysteries, *Science*, 2002, 296: 1618—1621.
11. Broecker, W. S., Ocean chemistry during glacial time, *Geochim. Cosmochim. Acta*, 1982, 46: 1689—1706.
12. Anderson, R. F., Chase, Z., Fleisher, M. Q. et al., The Southern Ocean's biological pump during the Last Glacial Maximum, *Deep Sea Res. II*, 2002, 49: 1909—1938.
13. Jansen, H., Modelling the marine carbonate pump and its implications on the atmospheric CO₂ concentration, Bremen: Universität Bremen (Dissertation), 2001, 1—128.
14. Broecker, W. S., Sanyal, A., Magnitude of the CaCO₃ dissolution events making the onset of times of glaciation, *Paleoceanography*, 1997, 12: 530—532.
15. Broecker, W. S., Clark, E., Glacial-to-Holocene redistribution of carbonate ion in the deep sea, *Science*, 2001, 294: 2152—2155.
16. Anderson, D. M., Archer, D., Glacial-interglacial stability of ocean pH inferred from foraminifer dissolution rates, *Nature*, 2002, 416: 70—73.
17. Keir, R. S., Berger, W. H., Atmospheric CO₂ content in the last 120,000 years: the phosphate-extraction model, *J. Geophys. Res.*, 1983, 88: 6027—6038.
18. Peterson, L. C., Prell, W. L., Carbonate preservation and rates of climatic change: an 800 kyr record from the Indian Ocean (eds. Sundquist, E. T., Broecker, W. S.), *The Carbon Cycle and Atmospheric CO₂: Natural Variations Archean to Present*, Washington, D. C.: AGU, *Geophys. Monogr.* 32, 1985, 251—269.
19. Wu, G., Yasuda, M. K., Berger, W. H., Late Pleistocene carbonate

- stratigraphy on Ontong-Java Plateau in the western equatorial Pacific, *Mar. Geol.*, 1991, 99: 135—150.
20. Le, J., Shackleton, N. J., Carbonate dissolution fluctuations in the western equatorial Pacific during the Late Quaternary, *Paleoceanography*, 1992, 7: 21—42.
 21. Curry, W. B., Lohmann, G. P., Late Quaternary carbonate sedimentation at the Sierra Leone Rise (eastern equatorial Atlantic Ocean), *Mar. Geol.*, 1986, 70: 223—250.
 22. Hodell, D. A., Charles, C. D., Sierro, F. J., Late Pleistocene evolution of the ocean's carbonate system, *Earth Planet. Sci. Lett.*, 2001, 192: 109—124.
 23. Sanyal, A., Hemming, N. G., Hanson, G. N. et al., Evidence for a higher pH in the glacial ocean from boron isotopes in foraminifera, *Nature*, 1995, 373: 234—236.
 24. Wang, H., Jain, Z., Carbonate dilution cycles in the late Quaternary South China Sea (eds. Ye, Z., Wang, P.), *Contributions to Late Quaternary Paleocyanography of the South China Sea* (in Chinese with English abstract), Qingdao: Qingdao Ocean Univ. Press, 1992, 283—294.
 25. Wang, P., Prell, W. L., Blum, P. et al., *Proceedings of the ODP, Initial Reports 184*, College Station: Ocean Drilling Program, Texas A&M University, 2000, 1—103 [CD-ROM].
 26. Rottmann, M. L., Dissolution of planktonic foraminifera and pteropods in South China Sea sediments, *J. Foraminiferal Res.*, 1979, 9: 41—49.
 27. Miao, Q. R., Thunell, C., Anderson, D. M., Glacial-Holocene carbonate dissolution and sea surface temperatures in the South China and Sulu seas, *Paleoceanography*, 1994, 9: 269—290.
 28. Hanebuth, T., Statterger, K., Grootes, P. M., Rapid flooding of the Sunda Shelf: A late-glacial sea-level record, *Science*, 2000, 288: 1033—1035.
 29. Thunell, R. C., Miao, Q., Calvert, S. E. et al., Glacial-Holocene biogenic sedimentation patterns in the South China Sea: Productivity variations and surface water pCO₂, *Paleoceanography*, 1992, 7: 143—162.
 30. Wang, P., Tian, J., Cheng, X., Transition of Quaternary glacial cyclicity in deep-sea records at Nansha, the South China Sea, *Science in China, Ser. D*, 2001, 44(10): 926—933.
 31. Shackleton, N. J., Berger, A., Peltier, W. R., An alternative astronomical calibration of the lower Pleistocene timescale based on ODP Site 677, *Transactions of the Royal Society of Edinburgh: Earth Sciences*, 1990, 81: 251—261.
 32. Tian, J., Wang, P., Cheng, X. et al., Astronomically tuned Plio-Pleistocene benthic $\delta^{18}\text{O}$ record from South China Sea and Atlantic-Pacific comparison, *Earth Planet. Sci. Lett.*, 2002, 203: 1015—1029.
 33. Jones, A., Kaiteris, P., A vacuum gasometric technique for rapid and precise analysis of calcium carbonate in sediments and soils, *J. Sediment. Petrol.*, 1983, 53: 655—660.
 34. Howard, W. R., Prell, W. L., Late Quaternary CaCO₃ production and preservation in the Southern Ocean: Implications for oceanic and atmospheric carbon cycling, *Paleoceanography*, 1994, 9: 453—482.
 35. Howell, P., ARAND time series and spectral analysis package for the Macintosh, Brown University, IGBP PAGES/World Data Center for Paleoclimatology Data Contribution Series #2001-044, Boulder, Colorado, USA: NOAA/NGDC Paleoclimatology Program, 2001.
 36. Imbrie, J., Hays, J. D., Martinson, D. G. et al., The orbital theory of Pleistocene climate: A support from a revised chronology of the marine $\delta^{18}\text{O}$ record (eds. Berger, A., Imbrie, J.), *Milankovitch and Climate*, Mass: Hingham, 1984, 269—305.
 37. Ruddman, W. F., Pleistocene sedimentation in the equatorial Atlantic: Stratigraphy and faunal paleoclimatology, *Bull. Geol. Soc. Am.*, 1971, 82: 283—302.
 38. Wang, P., Min, Q., Bian, Y. et al., Planktonic foraminifera in the continental slope of the northern South China Sea during the last 130,000 years and their paleoceanographic implications, *Acta Geol. Sin.* (in Chinese and English abstract), 1986, 60: 215—225.
 39. Wang, P., Wang, L., Bian, Y. et al., Late Quaternary paleoceanography of the South China Sea: surface circulation and carbonate cycles, *Mar. Geol.*, 1995, 127: 145—165.
 40. Fischer, H., Wahlen, M., Smith, J. et al., Ice core records of atmospheric CO₂ around the last three glacial terminations, *Science*, 1999, 283: 1712—1714.

(Received September 12, 2002; accepted January 13, 2003)